Published in final edited form as:
Cancer Res. 2013 March 15; 73(6): 1689–1698. doi:10.1158/0008-5472.CAN-12-3391.

Earlier Detection of Breast Cancer with Ultrasound Molecular Imaging in a Transgenic Mouse Model

Sunitha V. Bachawal[1], **Kristin C. Jensen**[2], **Amelie M. Lutz**[1], **Sanjiv S. Gambhir**[1], **Francois Tranquart**[3], **Lu Tian**[4], and **Jürgen K. Willmann**[1]

[1]Department of Radiology, Molecular Imaging Program at Stanford, Stanford University School of Medicine, Stanford, California, USA [2]Departments of Pathology, Stanford University, Stanford, California, USA and Veterans Affairs Palo Alto Health Care System [3]Bracco Suisse SA, Geneva, Switzerland [4]Department of Health, Research & Policy, Stanford University, Stanford, California, USA

Abstract

While there is an increasing role of ultrasound for breast cancer screening in patients with dense breast, conventional anatomical-ultrasound lacks sensitivity and specificity for early breast cancer detection. In this study we assessed the potential of molecular-ultrasound imaging, using clinically-translatable vascular endothelial growth factor receptor (VEGFR2)-targeted microbubbles (MB_{VEGFR2}), to improve the diagnostic accuracy of ultrasound in earlier detection of breast cancer and ductal carcinoma in situ (DCIS) in a transgenic mouse model (FVB/N-Tg(MMTV-PyMT)634Mul). *In vivo* binding specificity studies (n=26 tumors) showed that ultrasound imaging signal was significantly higher ($P<0.001$) using MB_{VEGFR2} compared to non-targeted microbubbles and imaging signal significantly decreased ($P<0.001$) by blocking antibodies. Ultrasound molecular imaging signal significantly increased ($P<0.001$), when breast tissue (n=315 glands) progressed from normal (1.65±0.17 a.u.) to hyperplasia (4.21±1.16), DCIS (15.95±1.31) and invasive cancer (78.1±6.31) and highly correlated with *ex vivo* VEGFR2 expression ($R^2=0.84$; 95% CI, 0.72, 0.91; $P<0.001$). At an imaging signal threshold of 4.6 a.u., ultrasound molecular imaging differentiated benign from malignant entities with a sensitivity of 84% (95% CI, 78, 88) and specificity of 89% (95% CI, 81, 94). In a prospective screening trail (n=63 glands) diagnostic performance of detecting DCIS and breast cancer was assessed and two independent readers correctly diagnosed malignant disease in >95% of cases and highly agreed between each other (ICC=0.98; 95% CI, 97, 99). These results suggest that VEGFR2-targeted ultrasound molecular imaging allows highly accurate detection of DCIS and breast cancer in transgenic mice and may be a promising approach for early breast cancer detection in women.

Corresponding Author Jürgen K. Willmann, M.D., Department of Radiology, Molecular Imaging Program at Stanford, School of Medicine, Stanford University, 300 Pasteur Drive, Room H1307, Stanford, CA 94305-5621, P: 650-723-5424; Fax: 650-723-1909, willmann@stanford.edu.

Conflicts of interest: FT is an employee of Bracco. KJ has served as a consultant for Clarient/GE. SG and JW have served as a consultant for Bracco.

Authors' Contributions

Conception and design: Jürgen K. Willmann, MD; Sunitha V. Bachawal, PhD
Development of methodology: Jürgen K. Willmann, MD; Sunitha V. Bachawal, PhD
Acquisition of data: Sunitha V. Bachawal, PhD, Kristin Jensen, MD, Amelie M. Lutz, MD; Jürgen K. Willmann, MD
Analysis and interpretation of data: Sunitha V. Bachawal, PhD; Kristin Jensen, MD, Amelie M. Lutz, MD; Lu Tian, PhD; Jürgen K. Willmann, MD
Writing, review and/or revision of the manuscript: All authors
Administrative, technical, or material support: Francois Tranquart, MD PhD; Sanjiv S. Gambhir, MD PhD
Study supervision: Jürgen K. Willmann, MD

Keywords

Targeted ultrasound imaging; VEGFR2; breast cancer; early detection; microbubbles

INTRODUCTION

Breast cancer is the most common cancer diagnosed in women in the USA, and the second leading cause of death from cancer in women (1). The American Cancer Society estimates 229,060 new diagnoses of breast cancer and 39,920 deaths from this cancer in 2012 in the USA (1). Earlier detection can substantially reduce deaths from breast cancer. Screening mammography, currently the most frequently performed imaging procedure for breast cancer screening, has been shown to decrease mortality by 22% in women 50 years or older, and by 15% in women 40 to 49 years (2).

However, diagnostic accuracy of mammography in detecting breast cancer is reduced in women with dense breasts. More than 50% of women younger than 50 years have either heterogeneously dense or very dense breast tissue, as do at least one third of women older than 50 years (3). In women with dense breast tissue, mammographic sensitivity regarding cancer detection can be as low as 30% to 48% (4, 5) with much higher interval cancer rates (5, 6) and worse prognosis in subsequent clinically detected cancers (7). Therefore, recent studies have addressed the value of adding ultrasound imaging to screening mammography (4, 8-12). A multi-center study of 2,637 women at increased risk for breast cancer with dense breast tissue showed that breast cancer was diagnosed on ultrasound alone in 12 of 40 patients (30%) (7). However, the positive predictive value (PPV) of ultrasound for cancer detection in that study was only 8.6%, resulting in a large number of unnecessary callbacks and biopsies (7). In addition, the sensitivity of ultrasound performed alone in detecting invasive breast cancer was only 50% (7) and even lower (27%) in another prospective multimodality screening study of 609 asymptomatic high risk women (13). These findings underscore that further improvements in ultrasound are critically needed to increase its accuracy in diagnosing malignant precursor or invasive breast cancer lesions, should it be included as a complementary imaging modality into breast cancer screening protocols.

Ultrasound molecular imaging combines the advantages of ultrasound with the capabilities of molecular imaging to visualize molecular signatures with high sensitivity and specificity *in vivo* (14, 15). Microbubble (MB) contrast agents already in clinical use with ultrasound can be further chemically modified to accumulate at vascular endothelial cells over-expressing molecular markers associated with either precursor lesions or invasive cancer (14, 16, 17). Vascular endothelial growth factor receptor type 2 (VEGFR2), a transmembrane receptor tyrosine kinase, is a well-studied molecular marker overexpressed on angiogenic vascular endothelial cells of cancer (18, 19). Several studies have demonstrated increased angiogenesis and VEGFR2 over-expression in invasive breast cancer in human breast cancer tissues (19-21). Recent immunohistochemistry studies suggest increased angiogenesis even at the precursor ductal carcinoma in situ (DCIS) stage (22). Ultrasound molecular imaging of VEGFR2 expression on angiogenic vessels in DCIS and invasive breast cancer may therefore be a promising new approach for improving diagnostic accuracy of ultrasound in earlier detection of precursor lesions and breast cancer.

In our study, we evaluated how ultrasound molecular imaging can depict different histological stages of breast cancer development, including mammary hyperplasia, DCIS, and invasive breast cancer, in the well-established FVB/N-Tg(MMTV-PyMT)634Mul transgenic mouse model (23-25) by using a new, clinical-grade VEGFR2-targeted contrast MB. In a prospective screening trial of transgenic and control mice we show that DCIS and

invasive breast cancer can be detected with high diagnostic accuracy and reliability by ultrasound molecular imaging.

MATERIALS AND METHODS

Transgenic Mouse Model

All procedures involving the use of laboratory animals were approved by the Institutional Administrative Panel on Laboratory Animal Care at Stanford University. A transgenic mouse model of breast cancer (FVB/N-Tg(MMTV-PyMT)634Mul) was used for all experiments. In this model, the mammary epithelium transforms into different histological stages of breast cancer development, similar to disease progression in humans, including mammary hyperplasia, ductal carcinoma in situ (DCIS), and invasive carcinoma (24, 25).

Design of Microbubbles

A novel clinical-grade VEGFR2-targeted microbubble contrast agent (MB_{VEGFR2}) containing perfluorobutane and nitrogen (BR55; synthesized under GMP by Bracco Suisse SA, Geneva, Switzerland), was prepared as described previously (26). Briefly, a heterodimeric peptide (5.5-kDa) that binds to VEGFR2 with high affinity (dissociation constant, K_D = 0.5 nmol/L) was conjugated with the amino group of DSPE-PEG2000-NH_2 (1,2-distearoyl-sn-glycerol-3-phosphoethanolamine-N-[amino (polyethylene glycol)-2000) to form VEGFR2-binding lipopeptides (27, 29). This lipopeptide construct was purified and incorporated into the phospholipid-based shell of MB (mean number of heterodimeric peptides per square micrometer on the MB shell: 34200 ± 1300; range, 31800 - 36600). The resultant product was lyophilized and stored in septum sealed vials. Before injection in mice, MB were reconstituted in 2 ml of 5% glucose. The mean diameter of MB_{VEGFR2} was 1.5 μm (range, 1-3 μm), as assessed by using a cell counter and sizer (Multisizer III Coulter Counter; Beckman Coulter, Fullerton, CA) (26). MB_{VEGFR2} was previously shown to cross-react with murine, rat, and human VEGFR2 (26, 30). Non-targeted MB that lack the VEGFR2 specific lipopeptide construct were used as control MB ($MB_{Control}$).

Ultrasound Molecular Imaging

Imaging Protocol—Ultrasound molecular imaging was performed as described previously (31) and a detailed description of the imaging protocol is provided in the Supplementary Materials. Images representing signal from adherent MB (molecular imaging signal) were displayed as color maps overlaid on B-mode images, automatically generated by using commercially available Vevo CQ software (VisualSonics, Toronto, Canada). The scale for the color maps was kept constant for all images.

***Binding Specificity of Microbubbles to VEGFR2* in Transgenic Mouse Model—** In the first part of the imaging study, VEGFR2 binding specificity of MB_{VEGFR2} was tested in 26 transgenic mice bearing tumors (Figure 1) in an intra-animal comparison study using MB_{VEGFR2} and $MB_{Control}$, as well as by performing *in vivo* competition experiments (details are provided in Supplementary Materials). To minimize any bias from repetitive injections in the same mice, injections were separated by at least 30 minutes waiting time to allow clearance of MB from previous injections (32).

Correlation Between *In Vivo* Imaging and Histology

Ultrasound Imaging—To determine how VEGFR2-targeted ultrasonic imaging signal varies in different histological stages of breast cancer progression (from normal mammary gland tissue to hyperplasia, DCIS and invasive breast cancer), in the second part of the study, the mammary glands of transgenic mice (n=233) and glands of age-matched control

litter mates (n=82) were imaged using MB_{VEGFR2} as described above at different stages of breast cancer development between ages 4 and 10 weeks, and the *in vivo* imaging signals were correlated with *ex vivo* histological findings (Figure 1). A total of 315 mammary glands were imaged and all mammary glands were excised immediately after imaging to allow direct correlation between *in vivo* imaging findings and *ex vivo* histology. Before isolating the mammary glands, the imaging plane (position of ultrasound transducer) was marked on the skin of the mammary gland using a tissue marking dye (Cancer Diagnostics, Inc., Morrisville, NC) to ensure that the imaged plane was correlated with about the same plane and oriented in the same way on *ex vivo* analysis.

Imaging Data Analysis—After each imaging session, the imaging data sets of all mice were analyzed offline in random order at a dedicated workstation with commercially available software (Visualsonics, Toronto, Ontario, Canada). Analysis was performed in a blinded fashion by one independent reader, blinded to the type of MB (MB_{VEGFR2} versus $MB_{Control}$), the age of the animals and the animal type (transgenic or control). Regions of interest (ROI) were drawn over the mammary gland and the magnitude of imaging signal from attached MB was assessed by calculating an average for pre- and post-destruction imaging signals and subtracting the average post-destruction signal from the average pre-destruction signal, as described previously (Figure 1) (33, 34).

Ex Vivo Analysis of Mammary Glands—*Ex vivo* analysis of mammary glands for quantitative immunofluorescence (QIF), and microvessel density (MVD) were performed using standard techniques (see Supplementary Materials).

Calculation of Ultrasonic Molecular Imaging Signal Thresholds

To determine thresholds of VEGFR2-targeted ultrasound imaging signals to allow discrimination of benign (normal and hyperplasia) from malignant histological entities (DCIS and invasive breast cancer) based on imaging, receiver operating characteristic (ROC) curves were constructed and the sensitivity and specificity for potential imaging signal threshold levels and corresponding 95% confidence intervals were calculated using the data sets from the above described imaging/histology correlation study from 315 mammary glands. Additionally, a non-parametric logistic regression model was used to predict the probability of a histological stage (normal, hyperplasia, DCIS or invasive breast cancer) based on ultrasound imaging. Based on these calculations, an imaging signal threshold level of 4.6 a.u. was selected to differentiate benign from malignant histological entities for the subsequent prospective imaging trial (see below).

Prospective Imaging Trial in Screening Setting

In the third part of the study, the diagnostic accuracy of ultrasonic molecular imaging in differentiating the four different histological tissues was assessed in a prospective screening setting (Figure 1). For this purpose, an additional 63 mammary glands from transgenic and wild type littermates at random ages between 4 and 10 weeks were scanned. This study design was chosen to simulate a screening scenario with “patients” with and without increased risk for breast cancer (transgenic and wild type littermates) that present with different mammary gland pathologies at the time of screening ultrasound. The imager was blinded to the age and group of mice (transgenic vs. normal) at the time of screening ultrasound. After each imaging exam, image analysis was performed as described above by two independent readers. Both readers were blinded to the age of the animals and the animal type (transgenic or control). Both readers were asked to render a diagnosis for each mammary gland (malignant versus benign) based on the ultrasonic molecular imaging signal obtained from the mammary gland and using the imaging signal threshold level of 4.6. a.u. as calculated above. The mammary glands were excised and *ex vivo* analysis of the

mammary glands was performed as described above. The diagnosis at pathology was used as reference standard to calculate diagnostic accuracy of ultrasound molecular imaging in diagnosing malignant versus benign disease in the prospective screening setting. One of the two readers performed a repeat analysis eight weeks after the first imaging analysis to assess intra-operator agreement.

Statistical Analysis

All data are represented as mean ± standard deviations. For details on statistical analysis please refer to Supplementary Methods.

RESULTS

Clinical-grade MB_{VEGFR2} bind to murine VEGFR2 in transgenic mice with high specificity

As a first step, we tested binding specificity of clinical grade MB_{VEGFR2} to murine VEGR2 in 26 breast cancers with different sizes in transgenic mice (mean diameter, 7 mm; range, 3 - 12 mm). Following intravenous administration of MB_{VEGFR2}, *in vivo* ultrasound imaging signal obtained from breast cancers was significantly higher ($P<0.001$) compared to the signal obtained after $MB_{Control}$ administration (Figure 2). In the same mice, binding specificity of MB_{VEGFR2} to VEGFR2 was further verified by *in vivo* blocking of the VEGFR2 receptor with anti-VEGFR2 antibody, which significantly ($P<0.001$) decreased the signal by 87% on average (Figure 2). Overall, these results confirmed *in vivo* binding specificity of clinical grade MB_{VEGFR2} to murine VEGFR2 in transgenic mice and demonstrated presence of increased VEGFR2 expression over a broad range of breast cancer tumor sizes.

Molecular ultrasound imaging signal increases as the mouse breast tissue progresses from normal to cancer

We then assessed the *in vivo* ultrasound molecular imaging signal in 315 mammary glands randomly scanned at different ages between weeks 4 and 10. Figure 3 summarizes the distribution of the four histological types (normal, hyperplasia, DCIS, invasive cancer) among all mammary glands. At age 4 weeks, many mammary glands already showed histological features of hyperplasia or DCIS; 30% of the mammary glands showed normal mammary tissue at that age. Presence of hyperplasia peaked in week 5 (29% of mammary glands). DCIS was the predominant histological feature between weeks 4 and 8 with a peak at week 7. Invasive breast cancer was first noted at week 7 and by week 10, 94% of mammary glands showed histological features of invasive breast cancer.

As the mammary glands progressed through the different histological types, ultrasound molecular imaging signal significantly increased ($P<0.001$) and positively correlated with histology ($P<0.001$) (Figure 4A & 4B). Normal breast tissue showed only background imaging signal (mean, 1.65 ± 0.17 a.u.); imaging signal significantly increased in hyperplasia (mean, 4.21 ± 1.16 a.u.; $P=0.021$). When breast tissue further progressed from hyperplasia to DCIS, mean ultrasound molecular imaging significantly increased to 15.95 ± 1.31 a.u. ($P<0.001$). Imaging signal further significantly increased ($P<0.001$) when DCIS progressed to invasive breast cancer (78.1 ± 6.31 a.u.) (Figure 4A & 4B). Imaging signal in breast cancer was 47.3-fold higher compared to normal breast tissue, 18.6-fold higher compared to hyperplasia, and 4.9-fold higher compared to DCIS.

VEGFR2 expression increases with breast tissue progression from normal, hyperplasia, DCIS, to invasive breast cancer

Following ultrasound imaging, mice were sacrificed and tumors excised for *ex vivo* analysis. VEGFR2 expression was significantly increased ($P<0.001$) in hyperplasia, DCIS,

and invasive breast cancer compared to normal breast tissue, and was highest on the angiogenic vasculature of invasive breast cancer (Figure 5). Quantitative VEGFR2-based immunofluorescence signal strongly correlated with *in vivo* VEGFR2-targeted ultrasonic molecular imaging (R^2=0.84; 95% CI, 0.72, 0.91; P<0.001). In addition to higher VEGFR2 expression levels, MVD significantly (P≤0.001) increased in hyperplasia, DCIS, and invasive breast cancer compared to normal tissue, suggesting that increased *in vivo* VEGFR2-targeted imaging signal during breast tissue progression from normal to invasive breast cancer was caused by a combination of higher target expression per vessel and an increase in the overall number of vessels expressing the target VEGFR2. Using a linear regression model, the fitted equation reflecting the association between *in vivo* ultrasonic imaging signal, QIF, and MVD was: Ultrasound signal = 0.11*MVD +3.55*QIF-0.47. The quantitative value generated by this equation is referred to as the angiogenesis score, and represents a combination of the number of vessels expressing the VEGFR2 and VEGFR2 expression per vessel. The angiogenesis score significantly increased (P≤0.001) from normal to hyperplasia, DCIS or invasive subtypes of breast cancer in this transgenic mouse model (Supplementary Figure S1). The adjusted coefficient of correlation was 0.74 (95% CI, 0.51, 0.89; P≤0.001), suggesting good correlation between *in vivo* ultrasonic molecular imaging signal and both MVD and VEGFR2 expression levels on the vasculature.

Ultrasound molecular imaging allows detection of DCIS and invasive breast cancer with high diagnostic accuracy

Figure 6 shows the ROC curve to differentiate benign histological entities (normal and hyperplasia) from diagnosing those that need further clinical work-up (DCIS and invasive breast cancer) based on ultrasound molecular imaging signals obtained in 315 mammary glands. Overall, ultrasound allowed the differentiation of benign from malignant diseases with high diagnostic accuracy (AUC of 0.94). Sensitivities, specificities, and positive and negative predictive values to differentiate benign from malignant cases using different imaging signal threshold levels were calculated and are summarized in Supplementary Tables S1 and S2. At a threshold level of 4.6 a.u., benign and malignant histological entities were predicted to be diagnosed with a sensitivity of 84% (95% CI, 78, 88) and a specificity of 89% (95% CI, 81, 94) (Supplementary Table S1).

Using the threshold level of 4.6 a.u., two readers analyzed an additional 63 mammary glands in a prospective screening setting (20 glands each with normal, DCIS, and invasive cancer; 3 hyperplastic glands). In this trial, malignant lesions were differentiated from benign lesions with a sensitivity of 100% (95% CI, 91, 100) and a specificity of 87% (95% CI, 66, 97) for both readers, respectively (Table 1a). Both readers overcalled three benign findings (one normal mammary gland and two glands with hyperplasia) as malignant (Table 1b). Discrepancies between both readers were observed in only 2/63 cases (Table 1b), which corresponded to an excellent inter-observer agreement (ICC=0.98; 95% CI, 97, 99). Similarly, reproducibility in repeated analysis of ultrasound molecular imaging data sets after 8 weeks performed by one of the readers was high (ICC=0.96; 95% CI, 90, 98).

DISCUSSION

Our study showed that VEGFR2-targeted ultrasound imaging signal increases when mammary glands progress from normal tissue to hyperplasia, DCIS, and invasive breast cancer in a transgenic mouse model. At an ultrasound molecular imaging signal threshold level of 4.6 a.u., DCIS and invasive breast cancer can be differentiated from normal and hyperplastic mammary glands with high sensitivity and specificity. Our results suggest that VEGFR2-targeted contrast MB can increase the diagnostic accuracy of ultrasound in earlier detection of both breast cancer and its precursor lesion DCIS.

Ultrasound (7, 35, 36) and other imaging technologies such as MRI (37, 38) and PET (39) are currently being evaluated as adjunct screening modalities in patients with mammographically dense breasts since screening mammograms can miss breast cancer in more than 50% of patients with dense breast tissue (4, 5). In fact, in several states in the United States dense breast laws have recently been passed that mandate radiologists to specifically inform patients about the presence of dense breast tissue on mammograms, acknowledging the limited sensitivity of mammography in detecting breast cancer in these patients. However, the diagnostic accuracy of current ultrasound screening techniques in breast cancer detection is low (40).

We explored whether the diagnostic accuracy of ultrasound in earlier breast cancer detection could be improved by molecular imaging of tumor angiogenesis in a mouse model. To simulate the apparent progression of ductal breast adenocarcinoma from normal to hyperplasia, DCIS, and invasive breast cancer as observed in patients, and to quantify the ultrasound molecular imaging signal associated with these four histological stages, we used a transgenic mouse model that recapitulates this progression in murine mammary glands. We found that the angiogenic switch, the stage at which angiogenesis occurs in tumor progression, can already be observed to some extent in hyperplasia. Presence of angiogenesis further increased significantly when mouse mammary glands developed DCIS and invasive cancer; the highest values of MVD and VEGFR2 were observed in mammary glands with invasive breast cancer. In accordance with our findings in transgenic mice, recent immunohistochemical studies in human breast samples demonstrated an angiogenic initiation at the hyperplasia stage with a further increase of angiogenesis with the development of DCIS and invasion (22, 41).

We then confirmed our hypothesis that *in vivo* ultrasound molecular imaging signal using a contrast agent targeted at tumor angiogenesis significantly increases during breast cancer development by correlating *in vivo* ultrasonic molecular imaging findings with *ex vivo* histopathological findings in 315 mammary glands. Quantitative immunofluorescence showed that both the number of angiogenic vessels and the *ex vivo* expression levels of VEGFR2 per vessel strongly correlated with *in vivo* ultrasound molecular imaging signal across the four different breast histologies. Collectively, these findings indicate that tumor angiogenesis including over-expression of angiogenic markers such as VEGFR2 may play a significant role in breast cancer progression in this mouse model, and that imaging and quantification of tumor angiogenesis using VEGFR2-targeted ultrasound contrast agents could be leveraged to aid in the earlier detection of clinically relevant findings such as DCIS and invasive breast cancer by defining imaging signal threshold levels.

This was further tested in a blinded prospective screening trial by using newly defined ultrasound molecular imaging signal threshold levels. To simulate a clinical scenario with “patients” at risk to develop breast cancer, transgenic and wild-type mice were randomly selected at various ages and prospectively screened with ultrasound molecular imaging, followed by direct *ex vivo* correlation with the *in vivo* imaging results. Our results in 63 prospectively analyzed mammary glands showed that clinically actionable findings such as DCIS and invasive breast cancer can be detected with a sensitivity of up to 100%, which was higher than the predicted value of 84% obtained from the previous part of our study. An explanation of this high sensitivity is the observation that all 20 DCIS and 20 invasive breast cancer cases included in this prospective screening trial happened to show high levels of VEGFR2 and MVD and thus, the ultrasound molecular imaging signal was measured above the pre-selected threshold level value of 4.6 a.u.. Both readers highly agreed between each other in differentiating malignant from benign disease and the false positive rate was low, resulting in a PPV as high as 93%. This suggests that ultasound molecular imaging has the potential not only to increase detection rates of DCIS and breast cancer in a screening setting

but also to eventually decrease the currently high call back rate and high number of unnecessary biopsies.

We acknowledge several limitations of our study. First, we acknowledge that the fast progression of mammary tissue over several weeks in the transgenic mouse model may not reflect the usually slow development of breast cancer in patients. This rapid transition may have artificially over-stimulated angiogenesis and subsequently VEGFR2 expression in DCIS and invasive cancer in our study. Second, this mouse model does not develop other benign lesions beyond hyperplasia and additional studies are needed to assess whether ultrasound allows differentiation of those lesions from DCIS and breast cancer based on the magnitude of the molecular imaging signal. Third, the prevalence of DCIS and invasive breast cancer in our mouse screening trial was higher than that in a clinical screening population; this may have overestimated positive and negative predictive values for ultrasound molecular imaging. Fourth, the injected microbubble dose was used according to previous experience in ultrasound molecular imaging of mice (26, 33, 42). The contrast agent dosing when scaling to future first in man clinical trials need to be assessed and may differ compared to the dosing used in mice. Finally, we acknowledge that with the current imaging equipment available we scanned only a two-dimensional imaging plane from the center of the breast lesions. Ongoing research explores volumetric ultrasound molecular imaging approaches to assess the molecular signature from the entire three-dimensional extent of the target tissues.

In conclusion, our results suggest that ultrasound molecular imaging using a novel clinical-grade VEGFR2-targeted ultrasound contrast agent allows highly accurate and reliable detection of DCIS and breast cancer in a screening trial of transgenic mice. This study lays the foundation for further development of this promising imaging approach for earlier breast cancer detection and paves the way for translational clinical trials in the future.

Supplementary Material

Refer to Web version on PubMed Central for supplementary material.

Acknowledgments

Authors would like to thank Kira Foygel, PhD for her assistance in staining tissue sections. We also acknowledge the support by Timothy Doyle, PhD in the Small Animal Imaging Facility at Stanford University.

GRANT SUPPORT

This research was supported by the R01 CA155289-01A1 (JKW) and by a Developmental Cancer Research Award from the Stanford Cancer Center (JKW).

Abbreviations

MB	Microbubble
DCIS	ductal carcinoma in situ
VEGFR2	vascular endothelial growth factor receptor type 2
MB_{VEGFR2}	(VEGFR2)-targeted microbubbles
$MB_{Control}$	non-targeted microbubbles
MVD	microvessel density
QIF	quantitative immunofluorescence

PPV	positive predictive value
NPV	negative predictive value
ROC	receiver operating characteristic

REFERENCES

1. Siegel R, Naishadham D, Jemal A. Cancer statistics, 2012. CA Cancer J Clin. 2012; 62:10–29. [PubMed: 22237781]
2. Humphrey LL, Helfand M, Chan BK, Woolf SH. Breast cancer screening: a summary of the evidence for the U.S. Preventive Services Task Force. Ann Intern Med. 2002; 137:347–60. [PubMed: 12204020]
3. Stomper PC, D'Souza DJ, DiNitto PA, Arredondo MA. Analysis of parenchymal density on mammograms in 1353 women 25-79 years old. AJR Am J Roentgenol. 1996; 167:1261–5. [PubMed: 8911192]
4. Kolb TM, Lichy J, Newhouse JH. Comparison of the performance of screening mammography, physical examination, and breast US and evaluation of factors that influence them: an analysis of 27,825 patient evaluations. Radiology. 2002; 225:165–75. [PubMed: 12355001]
5. Mandelson MT, Oestreicher N, Porter PL, White D, Finder CA, Taplin SH, et al. Breast density as a predictor of mammographic detection: comparison of interval- and screen-detected cancers. J Natl Cancer Inst. 2000; 92:1081–7. [PubMed: 10880551]
6. Boyd NF, Guo H, Martin LJ, Sun L, Stone J, Fishell E, et al. Mammographic density and the risk and detection of breast cancer. N Engl J Med. 2007; 356:227–36. [PubMed: 17229950]
7. Berg WA, Blume JD, Cormack JB, Mendelson EB, Lehrer D, Bohm-Velez M, et al. Combined screening with ultrasound and mammography vs mammography alone in women at elevated risk of breast cancer. JAMA. 2008; 299:2151–63. [PubMed: 18477782]
8. Buchberger W, Niehoff A, Obrist P, DeKoekkoek-Doll P, Dunser M. Clinically and mammographically occult breast lesions: detection and classification with high-resolution sonography. Semin Ultrasound CT MR. 2000; 21:325–36. [PubMed: 11014255]
9. Crystal P, Strano SD, Shcharynski S, Koretz MJ. Using sonography to screen women with mammographically dense breasts. AJR Am J Roentgenol. 2003; 181:177–82. [PubMed: 12818853]
10. Gordon PB, Goldenberg SL. Malignant breast masses detected only by ultrasound. A retrospective review. Cancer. 1995; 76:626–30. [PubMed: 8625156]
11. Leconte I, Feger C, Galant C, Berliere M, Berg BV, D'Hoore W, et al. Mammography and subsequent whole-breast sonography of nonpalpable breast cancers: the importance of radiologic breast density. AJR Am J Roentgenol. 2003; 180:1675–9. [PubMed: 12760942]
12. Kaplan SS. Clinical utility of bilateral whole-breast US in the evaluation of women with dense breast tissue. Radiology. 2001; 221:641–9. [PubMed: 11719658]
13. Weinstein SP, Localio AR, Conant EF, Rosen M, Thomas KM, Schnall MD. Multimodality Screening of High-Risk Women: A Prospective Cohort Study. J Clin Oncol. 2009
14. Pysz MA, Willmann JK. Targeted contrast-enhanced ultrasound: an emerging technology in abdominal and pelvic imaging. Gastroenterology. 2011; 140:785–90. [PubMed: 21255573]
15. Kiessling F, Bzyl J, Fokong S, Siepmann M, Schmitz G, Palmowski M. Targeted ultrasound imaging of cancer: an emerging technology on its way to clinics. Curr Pharm Des. 2012; 18:2184–99. [PubMed: 22352772]
16. Deshpande N, Needles A, Willmann JK. Molecular ultrasound imaging: current status and future directions. Clin Radiol. 2010; 65:567–81. [PubMed: 20541656]
17. Klibanov AL. Ligand-carrying gas-filled microbubbles: ultrasound contrast agents for targeted molecular imaging. Bioconjug Chem. 2005; 16:9–17. [PubMed: 15656569]
18. Hicklin DJ, Ellis LM. Role of the vascular endothelial growth factor pathway in tumor growth and angiogenesis. J Clin Oncol. 2005; 23:1011–27. [PubMed: 15585754]

19. Kranz A, Mattfeldt T, Waltenberger J. Molecular mediators of tumor angiogenesis: enhanced expression and activation of vascular endothelial growth factor receptor KDR in primary breast cancer. Int J Cancer. 1999; 84:293–8. [PubMed: 10371349]
20. Nakopoulou L, Stefanaki K, Panayotopoulou E, Giannopoulou I, Athanassiadou P, Gakiopoulou-Givalou H, et al. Expression of the vascular endothelial growth factor receptor-2/Flk- 1 in breast carcinomas: correlation with proliferation. Hum Pathol. 2002; 33:863–70. [PubMed: 12378509]
21. Price DJ, Miralem T, Jiang S, Steinberg R, Avraham H. Role of vascular endothelial growth factor in the stimulation of cellular invasion and signaling of breast cancer cells. Cell Growth Differ. 2001; 12:129–35. [PubMed: 11306513]
22. Carpenter PM, Chen WP, Mendez A, McLaren CE, Su MY. Angiogenesis in the Progression of Breast Ductal Proliferations. Int J Surg Pathol. 2009
23. Hutchinson JN, Muller WJ. Transgenic mouse models of human breast cancer. Oncogene. 2000; 19:6130–7. [PubMed: 11156526]
24. Guy CT, Cardiff RD, Muller WJ. Induction of mammary tumors by expression of polyomavirus middle T oncogene: a transgenic mouse model for metastatic disease. Mol Cell Biol. 1992; 12:954–61. [PubMed: 1312220]
25. Lin EY, Jones JG, Li P, Zhu L, Whitney KD, Muller WJ, et al. Progression to malignancy in the polyoma middle T oncoprotein mouse breast cancer model provides a reliable model for human diseases. Am J Pathol. 2003; 163:2113–26. [PubMed: 14578209]
26. Pysz MA, Foygel K, Rosenberg J, Gambhir SS, Schneider M, Willmann JK. Antiangiogenic cancer therapy: monitoring with molecular US and a clinically translatable contrast agent (BR55). Radiology. 2010; 256:519–27. [PubMed: 20515975]
27. Tardy I, Pochon S, Theraulaz M, Emmel P, Passantino L, Tranquart F, et al. Ultrasound molecular imaging of VEGFR2 in a rat prostate tumor model using BR55. Invest Radiol. 2010; 45:573–8. [PubMed: 20808233]
28. Pillai R, Marinelli ER, Fan H, Nanjappan P, Song B, von Wronski MA, et al. A Phospholipid-PEG2000 Conjugate of a Vascular Endothelial Growth Factor Receptor 2 (VEGFR2)-Targeting Heterodimer Peptide for Contrast-Enhanced Ultrasound Imaging of Angiogenesis. Bioconjug Chem. 2010
29. Shrivastava A, von Wronski MA, Sato AK, Dransfield DT, Sexton D, Bogdan N, et al. A distinct strategy to generate high-affinity peptide binders to receptor tyrosine kinases. Protein Eng Des Sel. 2005; 18:417–24. [PubMed: 16087652]
30. Bzyl J, Lederle W, Rix A, Grouls C, Tardy I, Pochon S, et al. Molecular and functional ultrasound imaging in differently aggressive breast cancer xenografts using two novel ultrasound contrast agents (BR55 and BR38). Eur Radiol. 2011; 21:1988–95. [PubMed: 21562807]
31. Deshpande N, Lutz AM, Ren Y, Foygel K, Tian L, Schneider M, et al. Quantification and monitoring of inflammation in murine inflammatory bowel disease with targeted contrast-enhanced US. Radiology. 2012; 262:172–80. [PubMed: 22056689]
32. Willmann JK, Cheng Z, Davis C, Lutz AM, Schipper ML, Nielsen CH, et al. Targeted microbubbles for imaging tumor angiogenesis: assessment of whole-body biodistribution with dynamic micro-PET in mice. Radiology. 2008; 249:212–9. [PubMed: 18695212]
33. Willmann JK, Paulmurugan R, Chen K, Gheysens O, Rodriguez-Porcel M, Lutz AM, et al. US imaging of tumor angiogenesis with microbubbles targeted to vascular endothelial growth factor receptor type 2 in mice. Radiology. 2008; 246:508–18. [PubMed: 18180339]
34. Lindner JR, Song J, Xu F, Klibanov AL, Singbartl K, Ley K, et al. Noninvasive ultrasound imaging of inflammation using microbubbles targeted to activated leukocytes. Circulation. 2000; 102:2745–50. [PubMed: 11094042]
35. Youk JH, Kim EK. Supplementary screening sonography in mammographically dense breast: pros and cons. Korean J Radiol. 2010; 11:589–93. [PubMed: 21076583]
36. Nothacker M, Duda V, Hahn M, Warm M, Degenhardt F, Madjar H, et al. Early detection of breast cancer: benefits and risks of supplemental breast ultrasound in asymptomatic women with mammographically dense breast tissue. A systematic review. Bmc Cancer. 2009; 9:335. [PubMed: 19765317]

37. Berg WA, Zhang Z, Lehrer D, Jong RA, Pisano ED, Barr RG, et al. Detection of breast cancer with addition of annual screening ultrasound or a single screening MRI to mammography in women with elevated breast cancer risk. JAMA. 2012; 307:1394–404. [PubMed: 22474203]

38. Saslow D, Boetes C, Burke W, Harms S, Leach MO, Lehman CD, et al. American Cancer Society guidelines for breast screening with MRI as an adjunct to mammography. CA Cancer J Clin. 2007; 57:75–89. [PubMed: 17392385]

39. Garami Z, Hascsi Z, Varga J, Dinya T, Tanyi M, Garai I, et al. The value of 18-FDG PET/CT in early-stage breast cancer compared to traditional diagnostic modalities with an emphasis on changes in disease stage designation and treatment plan. Eur J Surg Oncol. 2012; 38:31–7. [PubMed: 21937190]

40. Kuhl CK, Schmutzler RK, Leutner CC, Kempe A, Wardelmann E, Hocke A, et al. Breast MR imaging screening in 192 women proved or suspected to be carriers of a breast cancer susceptibility gene: preliminary results. Radiology. 2000; 215:267–79. [PubMed: 10751498]

41. Bluff JE, Menakuru SR, Cross SS, Higham SE, Balasubramanian SP, Brown NJ, et al. Angiogenesis is associated with the onset of hyperplasia in human ductal breast disease. Br J Cancer. 2009; 101:666–72. [PubMed: 19623180]

42. Lee DJ, Lyshchik A, Huamani J, Hallahan DE, Fleischer AC. Relationship between retention of a vascular endothelial growth factor receptor 2 (VEGFR2)-targeted ultrasonographic contrast agent and the level of VEGFR2 expression in an in vivo breast cancer model. J Ultrasound Med. 2008; 27:855–66. [PubMed: 18499845]

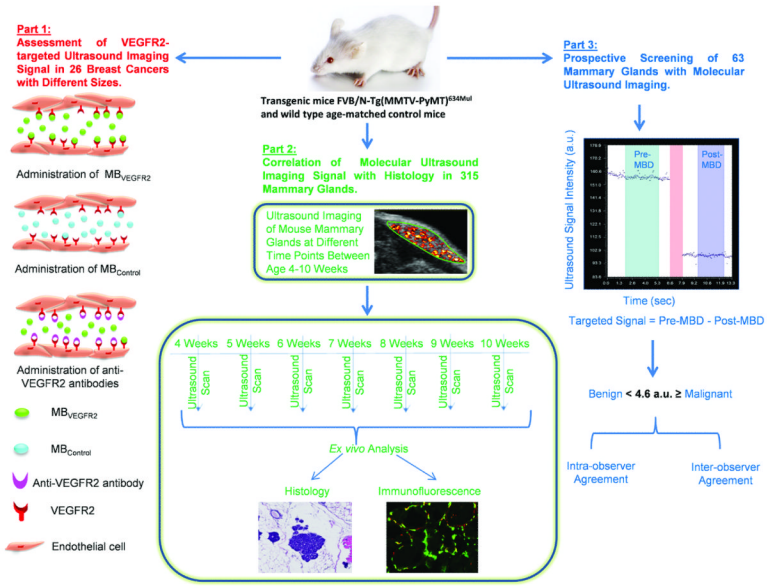

Figure 1.
Summary of overall study design which included three parts. MBD = microbubble destruction.

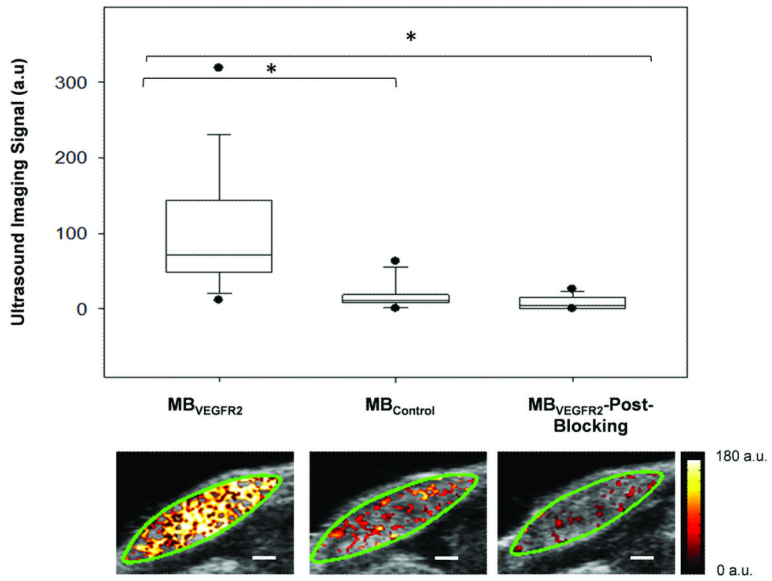

Figure 2.

Summary of ultrasound molecular imaging signals obtained from intra-animal comparison after intravenous administration of MB_{VEGFR2}, $MB_{Control}$ and MB_{VEGFR2} after blocking with anti-VEGFR2 antibodies (*P<0.001). Representative transverse B-mode images with overlaid VEGFR2-targeted ultrasound molecular imaging signals are shown from one mammary gland harboring invasive breast cancer. Green line represents region of interest (ROI). Scale bar = 1 mm.

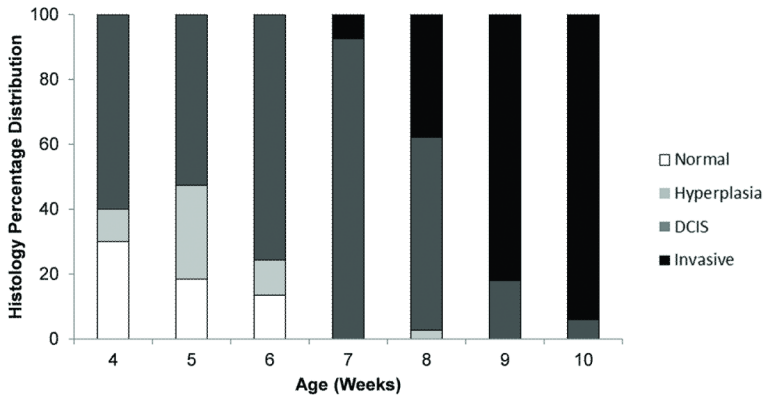

Figure 3.

Bar graph shows percentage distribution of four different histological findings (normal tissue, hyperplasia, DCIS, invasive breast cancer) in mammary glands of FVB/N-Tg(MMTV-PyMT)634Mul transgenic mouse model evaluated between age 4 and 10 weeks.

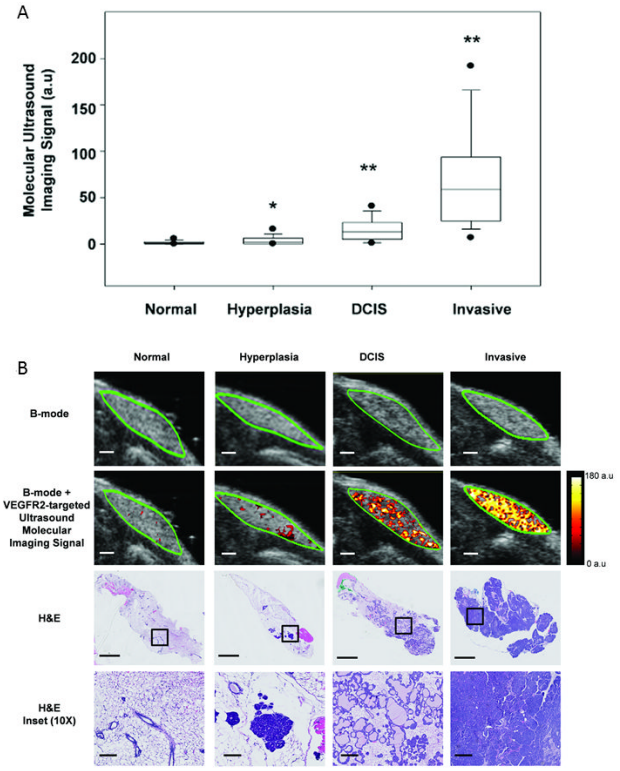

Figure 4.

(A) Box plot summarizes VEGFR2-targeted ultrasound molecular imaging signals obtained in normal, hyperplasia, DCIS and invasive breast cancer of 315 mammary glands. Imaging signal increased with mammary gland tissue progressing through different histological stages and imaging signals significantly increased compared to preceding stage. $*P = 0.021$; $**P < 0.001$). Note, each box in the plot represent the 25^{th} and 75^{th} quartiles, the line inside each box identifies the median and the vertical lines outside indicate the largest and smallest values in the series of measurements excluding the outliers. The 5^{th} and 95^{th} percentile of the data are represented as outliers (dots). **(B)** Representative ultrasound and H&E images of mammary glands with four different histological stages. Transverse B-mode with overlaid VEGFR2-targeted ultrasound molecular imaging signal (second row) shows substantial increase of ultrasound molecular imaging signal in DCIS and invasive breast cancer compared to hyperplasia and normal mammary gland tissue (scale bar = 1 mm). Note that B-mode images alone (first row) do not allow characterization of four different histological types. H&E staining of the corresponding mammary glands is shown in third row (scale bar = 1 mm). Ten-fold magnified images from insets are shown in fourth row (scale bar = 0.1 mm).

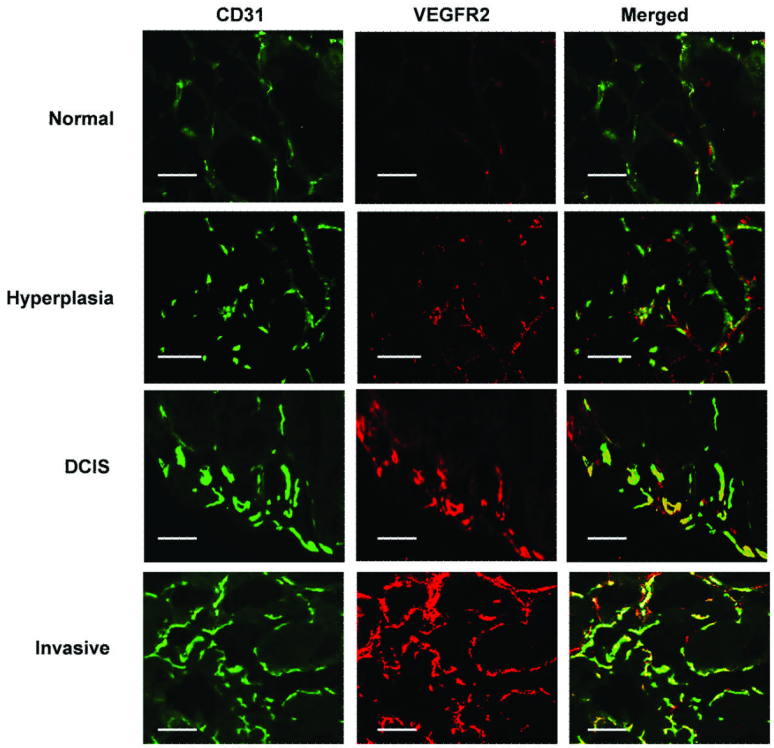

Figure 5.

Representative photomicrographs of mouse mammary glands with four different histological stages of breast cancer development. Mammary gland sections were stained for vascular endothelial cell marker CD31 (green, first column) and for VEGFR2 (red, second column). Merged images (yellow, third column) show expression of VEGFR2 on vascular endothelial cells. Note that number of microvessels and the VEGFR2 staining increased with breast cancer development (scale bar = 0.1 mm).

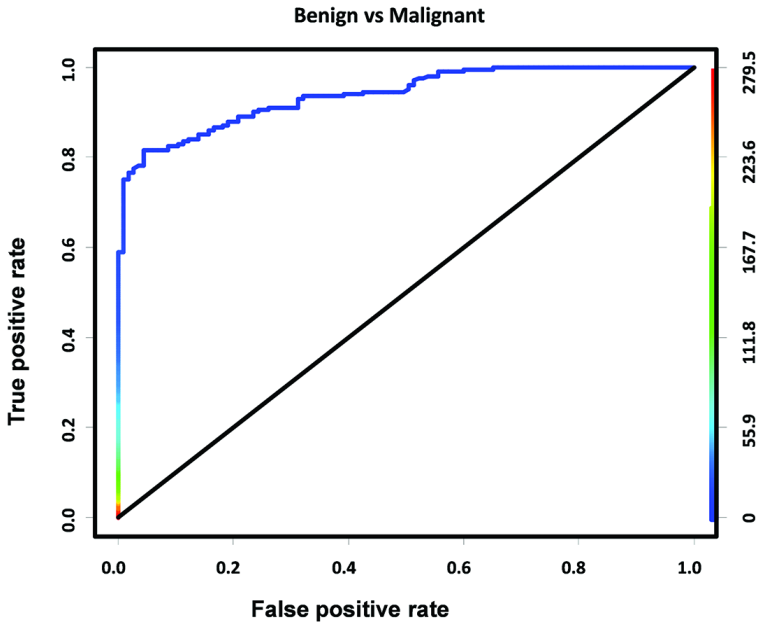

Figure 6.
ROC curve for differentiating benign histological entities (normal and hyperplasia) from malignant entities (DCIS and invasive cancer) at molecular ultrasound imaging threshold level of 4.6 a.u. Colored scale bar on right represents VEGFR2-targeted ultrasound molecular imaging signal in arbitrary units (a.u).

Table 1a

Sensitivity, Specificity, PPV and NPV in Diagnosing Malignant Disease (DCIS and Invasive Cancer) using an ultrasound Imaging Threshold Level of 4.6 a.u. in Prospective Imaging Trial in 63 Mammary Glands Analyzed by Two Independent Readers.

Ultrasound Imaging Threshold Level (a.u.)	Sensitivity (95% CI)	Specificity (95% CI)	PPV (95% CI)	NPV (95% CI)
4.6	100 (91 – 100)	87 (66 – 97)	93 (81 - 99)	100 (83 - 100)

Note: Values are identical for both readers since both readers misdiagnosed the same number of cases (see Table 1b).

Table 1b

Summary of Four (cases A – D) Out of 63 Cases with Discrepancies Between Prospective Ultrasound Imaging Diagnosis Provided by Two Independent Readers and Histological Findings.

Misdiagnosed Cases	Histological Finding	Ultrasound Signal Measured by Reader 1	Diagnosis by Reader 1	Ultrasound Signal Measured by Reader2	Diagnosis by Reader 2
A	Benign (Normal)	4.16	Benign	4.75	Malignant
B	Benign (Normal)	4.96	Malignant	0.57	Benign
C	Benign (Hyperplasia)	8.81	Malignant	4.67	Malignant
D	Benign (Hyperplasia)	11.87	Malignant	8.48	Malignant

Note: Both readers independently misdiagnosed 3/63 cases compared to histology using the ultrasound imaging threshold value of 4.6 a.u., corresponding to an error rate of 4.8%. Two cases (C and D) were overcalled as malignant by both readers; there was discrepancy between the two readers in two cases (A and B).